9-1-2001

C-band SAR backscatter characteristics of Arctic sea and land ice during winter

Konrad Steffen
University of Colorado Boulder

John Heinrichs
Fort Hays State University

Recommended Citation

Steffen, K., & Heinrichs, J. (2001). C-band SAR backscatter characteristics of Arctic sea and land ice during winter. Atmosphere-Ocean, 39(3), 289–299. https://doi.org/10.1080/07055900.2001.9649682

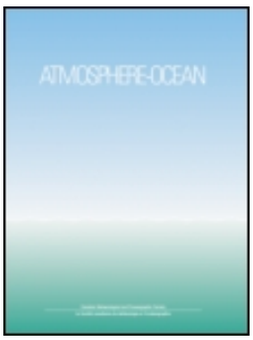

Atmosphere-Ocean

ISSN: 0705-5900 (Print) 1480-9214 (Online) Journal homepage: https://www.tandfonline.com/loi/tato20

C-band SAR backscatter characteristics of Arctic sea and land ice during winter

Konrad Steffen & John Heinrichs

To cite this article: Konrad Steffen & John Heinrichs (2001) C-band SAR backscatter characteristics of Arctic sea and land ice during winter, Atmosphere-Ocean, 39:3, 289-299, DOI: 10.1080/07055900.2001.9649682

To link to this article: https://doi.org/10.1080/07055900.2001.9649682

C-band SAR Backscatter Characteristics of Arctic Sea and Land Ice during Winter

Konrad Steffen[1,*] and John Heinrichs[2]

[1]*University of Colorado, Cooperative Institute for Research in Environmental Sciences*
Center for the Study of Earth from Space, and Department of Geography
Boulder, CO 80309-0216
[2]*Department of Geosciences, Fort Hays State University, Hays, KS*

[Original manuscript received 4 January 2000; in revised form 15 August 2000]

ABSTRACT *Synthetic Aperture Radar (SAR) data has become an important tool for studies of polar regions, due to high spatial resolution even during the polar night and under cloudy skies. We have studied the temporal variation of sea and land ice backscatter of twenty-four SAR images from the European Remote Sensing satellite (ERS-1) covering an area in Lady Ann Strait and Jones Sound, Nunavut, from January to March 1992. The presence of fast ice in Jones Sound and glaciers and ice caps on the surrounding islands provides an ideal setting for temporal backscatter studies of ice surfaces. Sample regions for eight different ice types were selected and the temporal backscatter variation was studied. The observed backscatter values for each ice type characterize the radar signatures of the ice surfaces. This time series of twenty-four SAR images over a 3-month period provides new insights into the degree of temporal variability of each surface. Ice caps exhibit the highest backscatter value of –3.9 dB with high temporal variability. Valley glacier ice backscatter values decrease with decreasing altitude, and are temporally the most stable, with standard deviations of 0.08–0.10 dB over the 90-day period.*

First-year ice and lead ice show a negative trend in backscatter values in time and a positive correlation of up to 0.59 with air temperature over the 90-day period. For first-year ice and lead ice, episodes of large temperature fluctuations (±12°C) are associated with rapid changes in backscatter values (±2 dB). We attribute the backscatter increase to a temperature-induced increase in brine volume at the base of the snow pack. Multi-year ice, conglomerate ice and shore ice are relatively stable over the 3-month period, with a backscatter variation of only a few dBs. An observed lag time of up to three days between backscatter increase/decrease and air temperature can be attributed to the insulation effect of the snow cover over sea ice. The net range of the backscatter values observed on the most temporally stable surface, valley glacier ice, of about 0.30 dB indicates that the ERS-1 SAR instrument exceeds the 1 dB calibration accuracy specified for the Alaska SAR Facility processor for the three winter months.

RÉSUMÉ *[Traduit par la rédaction] Les données des radars à ouverture synthétique (ROS) sont devenues un outil important pour l'étude des régions polaires, en raison de leur haute résolution spatiale même durant la nuit polaire et sous des ciels nuageux. Nous avons étudié la variation dans le temps de la rétrodiffusion de la glace de mer et de la glace terrestre sur 24 images ROS provenant du Satellite européen de télédétection (ERS-1) et couvrant la région des détroits Lady Ann et de Jones, au Nunavut, de janvier à mars 1992. La présence de banquise côtière dans le détroit de Jones ainsi que de glaciers et de calottes glacières sur les îles avoisinantes est particulièrement favorable aux études temporelles de rétrodiffusion des surfaces de glace. Nous avons sélectionné des régions échantillons pour 8 types de glace et étudié la variation dans le temps de leurs échos. Les valeurs de rétrodiffusion observées pour chaque type de glace caractérisent la signature radar des surfaces de glace. Cette série chronologique de 24 images sur une période de trois mois donne un éclairage nouveau sur le degré de variabilité temporelle de chaque surface. Ce sont les calottes glacières qui ont la plus forte valeur de rétrodiffusion, –3,9 dB, avec une variabilité temporelle élevée. Les valeurs de rétrodiffusion des glaciers de vallées diminuent avec l'altitude décroissante et sont les plus stables dans le temps, affichant un écart-type de 0,08–0,10 dB durant la période de 90 jours.*

Les valeurs de rétrodiffusion de la glace de première année et de la glace se formant dans les chenaux montrent une tendance négative dans le temps et une corrélation positive jusqu'à 0,59 avec la température de l'air sur la période 90 jours. Pour la glace de première année et de chenaux, les épisodes de grandes variations de température (±12°C) correspondent à des changements rapides dans les valeurs de rétrodiffusion (±2 dB). Nous attribuons cet accroissement de rétrodiffusion à une augmentation (de cause thermique) du volume de saumure à la base de la couche de neige. La glace de plusieurs années, les conglomérats de glace et la glace de rivage sont assez stables durant la période de trois mois, la variabilité de leurs échos n'étant que de quelques dB. Un décalage de jusqu'à trois jours observé entre l'augmentation ou la diminution de la rétrodiffusion et celle de la température de l'air peut être attribué à l'effet isolant de la couche de neige sur la glace de mer. L'intervalle net de 0,30 dB dans lequel varient les valeurs de rétrodiffusion observées pour les glaciers de vallées, qui présentent les surfaces les plus stables dans le temps, indique que le ROS du ERS-1 excède la précision d'étalonnage de 1 dB spécifiée pour le processeur du Alaska SAR Facility pour les trois mois d'hiver.

*Corresponding author's e-mail: koni@seaice.colorado.edu

1 Introduction

Monitoring sea ice in polar regions is essential for the understanding of climate processes. In particular, ice concentration and ice thickness are of interest because of their impact on energy exchanges at the ocean-atmosphere interface that affect Arctic climate. In this paper we examine the temporal variations of SAR backscatter for several types of sea and land ice with the intent of better understanding the processes at that interface.

The European Remote Sensing satellite (ERS-1), because of its 3-day repeat orbit (also called the ice cycle) during the months of January to March 1992, has the necessary temporal resolution required to study the evolution of the ice cover and its dynamic change due to weather or ocean currents. We analyze twenty-four Synthetic Aperture Radar (SAR) images for the backscatter variability of different ice types over a 3-month period and relate those changes to variations in air temperature recorded at the nearby Grise Fiord meteorological station on Ellesmere Island. Snowfall data from Grise Fiord showed no correlation with backscatter changes, which is not unexpected; spatial variability of snowfall and the redistribution of new snow by strong surface winds are the main causes. Thus, we have not discussed the snowfall analysis in the results section. SAR data are a useful tool in high latitude regions because data quality is maintained even in cloudy conditions and at night.

Previous studies have shown that first-year and old ice can be clearly separated based on their backscattering coefficient (Steffen and Heinrichs, 1994; Kwok and Cunningham, 1994). Further, it was shown that smooth first-year ice and rough first-year ice were not significantly different in the backscatter domain looking at a single image. In the following we provide temporal records of SAR backscatter variation for various sea-ice and land-ice types, and propose mechanisms to explain observed patterns.

2 Methods

A series of 24 ERS-1 SAR C-band (5.3 GHz) images covering Lady Ann Strait, which lies between Devon and Ellesmere Islands in the Canadian Arctic, was acquired from the Alaska SAR Facility (ASF). This area was chosen because of the large variety of land- and sea-ice surface types present. Each of the images represents a surface area of 100 km by 100 km at a spatial resolution of 100 m. The set of images covers the period 4 January to 23 March 1992 at intervals of three or six days (N=24). All of the images were taken on ascending passes of the ERS-1 satellite at the same time of day (between 02:22:33 and 02:22:46 UTC). The SAR data were extracted from tape, calibrated using the operational ASF algorithm (Kwok and Cunningham, 1994), converted to decibels (dB), and scaled to fit into raster images with one byte per pixel. The calibration error is specified to be less than 1 dB using the operational ASF algorithm and the noise correction constants supplied with the data (Williams, 1996).

For comparison with the SAR data, atmospheric data for Grise Fiord (Fig. 1) were acquired from the Meteorological Service of Canada (MSC). Grise Fiord is the closest meteorological station to Lady Ann Strait, lying at a distance of less than 40 km. The Grise Fiord data consist of the minimum, mean and maximum daily temperatures over the entire study period.

The sea ice west of the polynya in Jones Sound is landfast, resulting in the formation of an ice arch across Lady Ann Strait. The lack of motion in the fast ice allows us to study the change of backscatter with time. The position accuracy for ERS-1 SAR scenes of 500 m (five low-resolution image pixels) (Williams, 1996) is not sufficient to study temporal backscatter variability of ice floes or ice near the shore. Once the SAR images were visually coregistered to within ±5 pixels, we used a statistical approach to optimize the overlay. One image (Fig. 2) that includes the entire region of interest was selected as a reference. Several tie points (small high-contrast features on land or within the fast ice) were identified in the reference image and the coordinates of the corresponding features in each SAR image were used to calculate rough x and y offsets relative to the reference image. The offsets were then varied crosswise ±5 pixels, and for each setting the spatial correlation coefficient was derived between the image and the reference (Fig. 3). The correlation matrix ranged from 0.9991 to 0.9995. The linear offset with the maximum correlation was then used for the final coregistration. No image warping was conducted because the images were of almost identical areas along the same orbit, therefore, only a linear offset was required. The residual registration error between the images is expected to be less than 2 pixels. Despite an accurate coregistration, even a 1-pixel coregistration error can introduce spurious backscatter variability for small regions. To avoid this problem, areas, which had similar backscatter values (homogeneous areas with no backscatter gradient), were selected for each of six sea-ice and two land-ice types (Table 1, Fig. 2).

3 Results

We selected twenty-eight sampling regions representing eight different ice types: ice caps, valley glaciers, and sea ice, including multi-year ice, first-year ice, lead ice, low backscatter first-year ice, and near-shore ice. The selection of the ice types was based on visual inspection of the SAR images, such as feature identification of ice types (Steffen and Heinrichs, 1994), and characteristic temporal backscatter values of ice types (Kwok and Cunningham, 1994). No displacement was observed of the ice in any of the sampling regions during the study period, indicating that the observed temporal variability of backscatter is not related to ice motion. The backscatter characteristics of various types of land and sea ice and their variability with time are presented below.

a *Land Ice*

1 ICE CAPS (IC1-2)

Ice caps in the percolation zone are among the brightest natural radar reflectors on the earth, as a result of the presence of

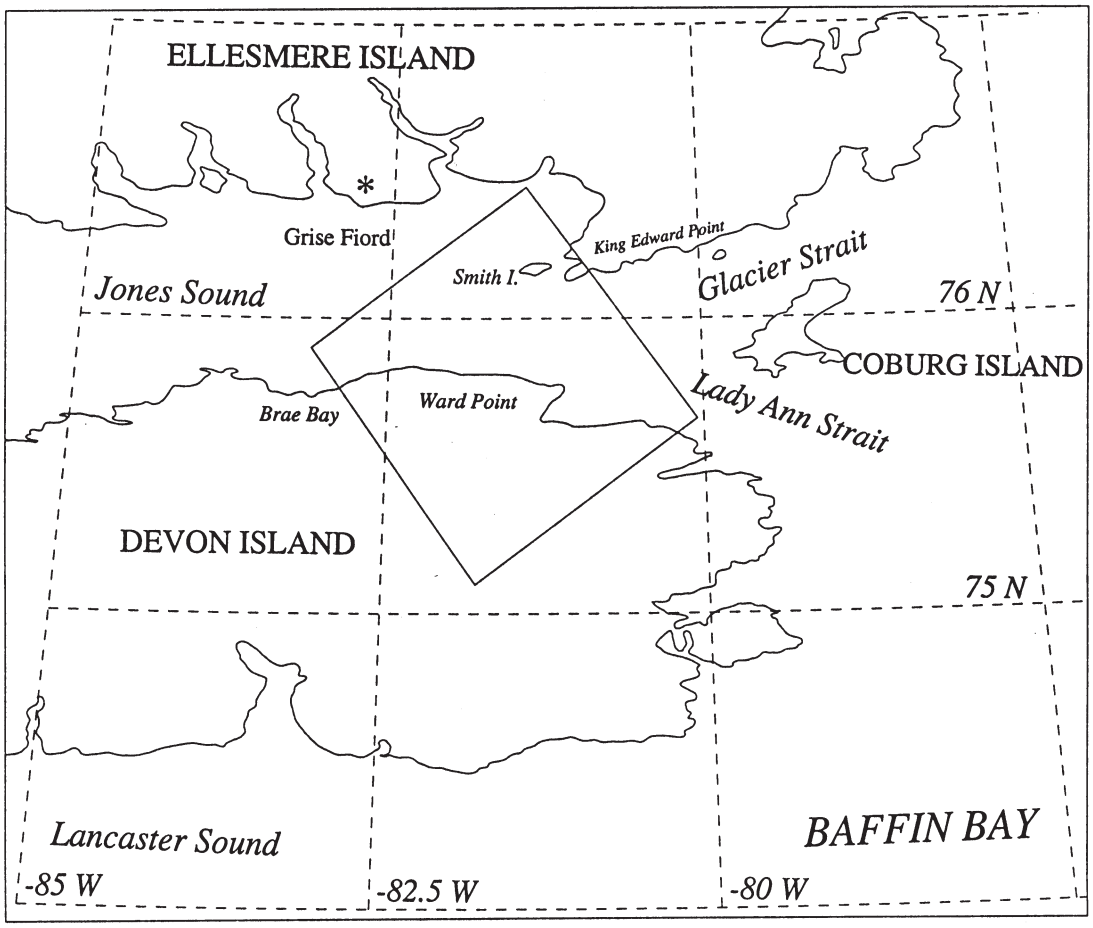

Fig. 1 The location of the twenty-four ERS-1 SAR images used in this study is shown in Lady Ann Strait, east of Jones Sound and west of Coburg Island.

solid ice bodies (glands, pipes, and lenses) within the firn (Jezek et al., 1993; Fahnestock at al., 1993; Rignot, 1995). Therefore it is not surprising that, of all ice types, the Devon ice cap exhibits the highest mean backscatter values of –4.0 dB and –3.7 dB, respectively (Table 1, Fig. 4). Similar ERS-1 SAR backscatter values of –3 dB to –4 dB were reported for the Svalbard ice caps (Rees et al., 1995). The two sample regions IC1 and IC2 at 600 and 1400 m above sea level are located in the percolation zone, where occasional summer melt water penetrates the snow and firn layers and refreezes. Jezek et al. (1994) observed a backscatter of –2 dB at an elevation of about 2100 m in the percolation facies along the western slope of the Greenland ice sheet. Their value is slightly higher than, but consistent with, the backscatter means of the Devon ice cap samples.

The temporal standard deviations of backscatter for the ice cap regions are –1.06 dB and –1.17 dB for IC1 and IC2 respectively, with spatial standard deviations around 0.5 dB (Table 1). Most of the variability is in the form of sudden jumps in backscatter values (Fig. 4). A possible explanation of the temporal backscatter variability for the Devon ice cap is the formation of surface hoar. A backscatter increase of 5 dB has been observed in relation to the development of hoar frost on ice caps in Alaska (Partington, 1998). Surface hoar is a layer of ice crystals from 1 mm to 10 mm in size that grows on a snow surface under certain conditions. These conditions include a temperature gradient of at least 5°C between the surface and the air (Colbeck, 1988), a negative surface radiation balance, a source of excess water vapour, and wind speeds between 1 m s^{-1} and 2 m s^{-1} (Hachikubo and Akitaya, 1997). These meteorological conditions are common on the ice caps surrounding Lady Ann Strait in winter (Müller et al., 1979).

2 GLACIER ICE (G1-3)

Eastern Glacier is a valley glacier fed by the surrounding ice caps on Devon Island. Three samples taken from the ablation area of this glacier have mean backscatter values of –9.8 dB to –13.7 dB (Table 1). The backscatter of the Devon Island glacier samples decreases with decreasing elevation (Table 1), which can be attributed to the transition from rough refrozen snow to a smoother ice surface at lower elevation.

The standard deviation for the glacier backscatter samples ranges from 0.08 dB to 0.10 dB over the study period, making this surface category the most stable of all those studied (Fig. 4). Our findings of low backscatter variability for glacier ice is consistent with laboratory measurements made by Swift et al. (1992), showing that air temperature has a negligible effect on the C-band backscatter of freshwater ice.

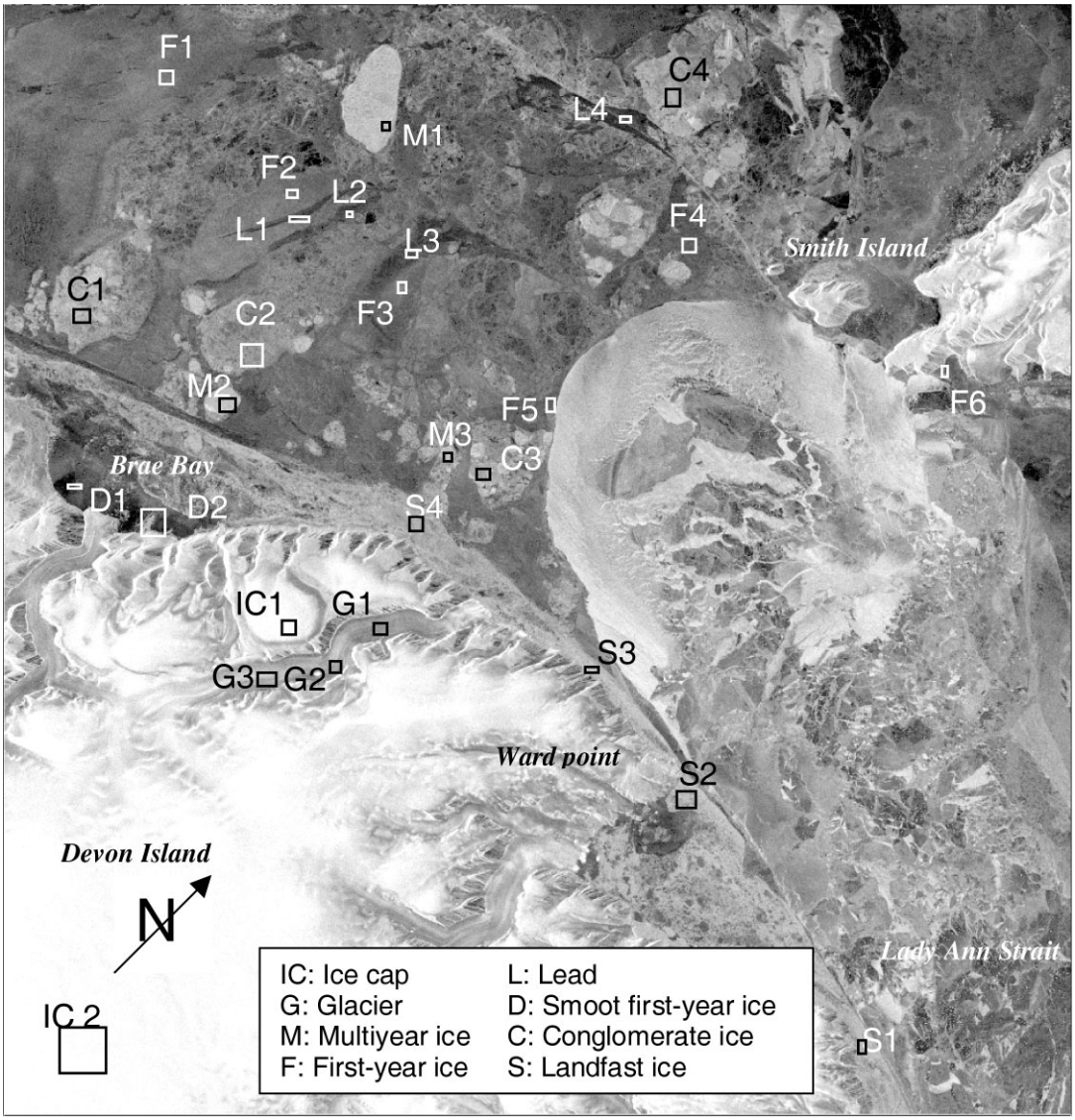

Fig. 2 ERS-1 SAR image acquired on 15 February 1992 (© European Space Agency, 1992). This image was the reference image used for coregistration and identification of the sample regions, which are indicated on the image.

The mean range between maximum and minimum backscatter values for all three glacier sites was 0.3 dB. The magnitude of this range suggests that the accuracy of the ERS-1 SAR instrument is within the calibration accuracy of 1 dB suggested by the ASF for the three winter months.

b Sea ice

1 MULTIYEAR ICE (M1-3)

The mean backscatter values for the three multi-year ice regions (M1 to M3) ranged from –9.4 dB to –9.8 dB (Table 1). These backscatter values are comparable to land-fast multi-year ice values of –9 dB to –9.5 dB found in Lancaster Sound near Resolute Bay during late winter and spring (Barber et al., 1995), and with multi-year ice values of –9 dB reported by Kwok and Cunningham (1994) for the eastern Beaufort Sea. Steffen and Heinrichs (1994) reported multi-year backscatter values of –10.2 dB and –11.0 dB in the Beaufort Sea for two days in April 1992.

The temporal variability of multi-year backscatter, with standard deviations ranging from 0.10–0.14 dB, is the lowest of all six sea-ice types in this study (Table 1). Barber et al. (1995) also found that landfast multi-year ice in winter and spring had the lowest temporal variability of backscatter for all sea-ice types. Kwok and Cunningham (1994) observed multi-year backscatter values within a 0.5 dB range through the winter for the Beaufort Sea, which is consistent with our observed range from 0.38 dB to 0.78 dB for the Lady Ann Strait over the 3-month period.

All of the multi-year samples have no significant trends over the 90-day period (Table 1). This can be explained by the dominant volume scattering from small gas bubbles (0.5–2.5 mm in size) in multi-year ice (Onstott, 1992). The dielectric loss factor (ε'') of multi-year ice is close to zero, since the ice is nearly salt-free (Hallikainen and Winebrenner, 1992), resulting in a penetration depth of C-band radiation of approximately 0.6 m (Schuchmann et al., 1991).

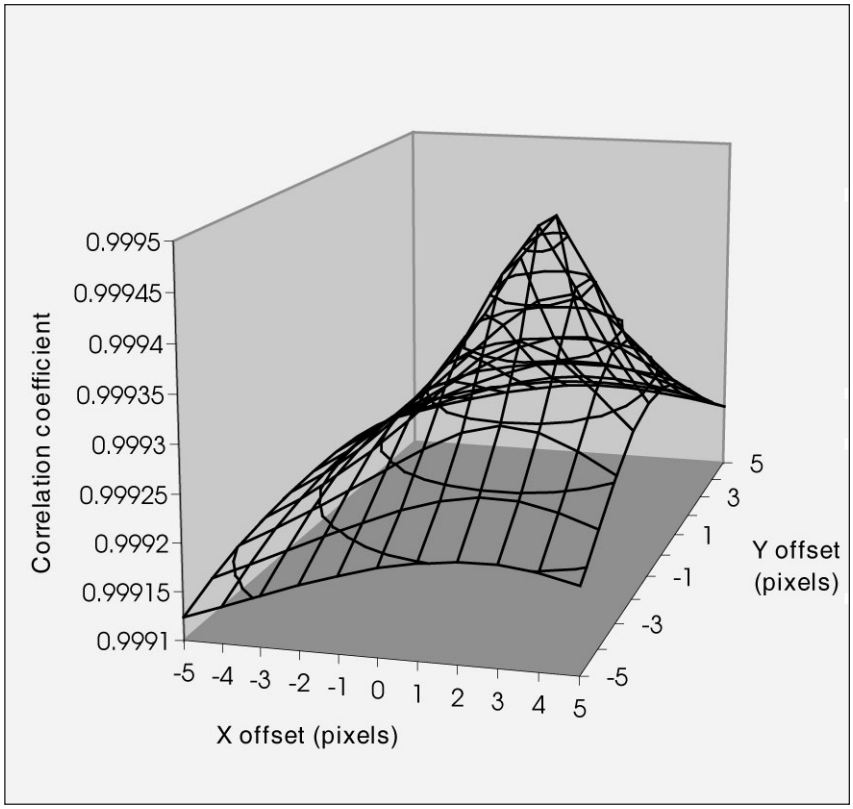

Fig. 3 An example of image to image correlation coefficients for linear offsets varied crosswise ±5 pixels. The two images compared in this figure were collected on 25 January and 15 February 1992.

2 FIRST-YEAR ICE (F1-6)

The six first-year ice samples have lower mean backscatter values (–15.6 dB to –18.5 dB) than any of the multi-year ice samples (Table 1). Using ERS-1 SAR data over the Beaufort Sea, Kwok and Cunningham (1994) measured backscatter means of –13.6 dB for deformed (ridged) first-year ice and –17.1 dB for undeformed first-year ice.

The first-year samples exhibit a high temporal backscatter variability with standard deviations between 0.63 dB and 1.23 dB (Table 1). The temporal variability is greater than that of the multi-year ice (Fig. 4). Further, the backscatter values show some correlation with Grise Fiord air temperatures (Fig. 5). Episodes of temperature fluctuations (±12ºC) are associated with rapid changes in backscatter values (±2 dB). Each rapid rise in backscatter is followed with a descent to the initial value within a few days. A lag of up to three days exists between the temperature and backscatter peaks. Each first-year ice sample depicts a positive correlation with the Grise Fiord temperature (Table 1), with a maximum value of 0.59. The positive correlation of first-year backscatter with air temperature for the same range (–20 to –40ºC) was also reported by Onstott (1992) and Barber et al. (1995).

The backscatter of first-year ice in Lady Ann Strait shows some long-term variability (Figs 4 and 5). First-year ice regions have, in general, significant negative trends at the 95% level over the entire 90-day time period, the largest being –0.033 dB day^{-1} at site F6 (Table 1). The main backscatter decrease occurred in January at the beginning of the study period. The dielectric constant and loss factor of first-year ice do not decrease monotonically with temperature. The relationship is more complicated and is influenced by salinity and geometry of brine inclusions (Shokr, 1998).

We attribute the short-term increase in backscatter to an increase in brine volume in the lower portion of the snow pack associated with an increase in the snow/ice interface temperature. Hallikainen and Winebrenner (1992) have asserted that liquid brine at the snow/ice interface is a major contributor to the backscatter signature of first-year ice and, with the increase of the insulating snow cover due to a higher snow/ice interface temperature, more liquid brine exists. The existence of a thin brine layer underneath rough saline snow has been shown to produce a large backscatter increase (Ulander et al., 1995). Liquid brine in the snow collects around the contact points of the snow crystals (Drinkwater and Crocker, 1988) and forms small disc-shaped inclusions (Swift et al., 1992). Provided the liquid fraction of brine is small (below 30–40%), the difference between the dielectric constants of brine-wetted snow and dry snow in the basal layer results in increased reflectivity at the air/snow interface and a corresponding increase of volume scattering (Drinkwater and Crocker, 1988; Ulander et al., 1995). Both processes meet the major criteria for explaining first-year ice

TABLE 1. Characteristics of the sample regions used to examine the variation of land-ice and sea-ice backscatter with time. For each sample region the ERS-1 SAR backscatter (σ^o) means, standard deviations, and trends are given. In addition, the backscatter (σ^o) correlation to minimum temperatures for Grise Fiord (GF) is shown.

Box ID	Description	Number of pixels	Mean σ° over 90 days (dB)	Stand. Dev. σ° over 90 days (dB)	Spatial Stand. Dev. σ° (dB)	σ° trend over 90 days (dB d^{-1})	Trend signif. at 95% level	σ° corr. w/GF min. temp.
IC1	Small ice dome on Devon Island	121	–4.0	1.06	0.49	–0.0148	No	–0.08
IC2	Main Devon Island ice cap	1680	–3.8	1.17	0.52	–0.0137	No	0.18
G1	Eastern Glacier on Devon Island	100	–13.7	0.10	0.93	–0.0006	No	–0.02
G2	Eastern Glacier on Devon Island	81	–11.7	0.09	1.02	0.0003	No	0.17
G3	Eastern Glacier on Devon Island	180	–9.8	0.08	1.69	0.0014	No	0.16
M1	SE portion of large MY floe	64	–9.4	0.10	0.76	–0.0014	No	–0.31
M2	Centre of small MY floe	132	–9.8	0.10	0.86	–0.0017	No	–0.34
M3	Very small MY piece	35	–9.6	0.14	0.97	–0.0013	No	–0.28
F1	FY ice well into Jones Sound	110	–15.6	0.79	0.80	–0.0102	No	0.55
F2	FY ice near large MY floe	90	–16.8	0.63	0.92	–0.0088	No	0.59
F3	FY ice closer to ice edge	72	–15.9	1.23	0.89	–0.0312	Yes	0.47
F4	FY ice N of polynya	132	–18.5	0.73	1.15	–0.0170	Yes	0.41
F5	FY ice along ice arch (furthest west)	78	–18.2	1.07	1.24	–0.0204	Yes	0.54
F6	FY ice just E of King Edward Point	120	–17.3	0.99	1.50	–0.0325	Yes	0.40
L1	Narrow refrozen lead	16	–19.8	1.55	0.76	–0.0056	No	0.28
L2	Very narrow refrozen lead	30	–18.5	0.64	1.46	–0.0088	No	0.35
L3	Centre of wide refrozen lead	56	–19.0	1.76	1.05	–0.0559	Yes	0.33
L4	Narrow lead N of polynya (near L6)	50	–20.6	1.10	1.49	–0.0258	Yes	0.37
D1	Low backscatter sea ice in Brae Bay	40	–23.7	1.14	0.99	0.0086	No	0.47
D2	Low-backscatter sea ice in Brae Bay	56	–22.5	0.85	2.39	–0.0020	No	0.66
C1	Conglomerate ice mass N of Brae Bay	168	–10.5	0.23	1.22	–0.0058	Yes	–0.40
C2	Conglomerate ice mass NE of Brae Bay	340	–13.8	0.24	1.18	–0.0076	Yes	–0.49
C3	Conglomerate ice mass N of Ward Point	90	–12.1	0.14	0.82	–0.0044	Yes	0.00
C4	Conglomerate ice mass N of polynya	195	–11.7	0.17	0.88	–0.0057	Yes	0.01
S1	Sea ice in shear zone off Devon Island	77	–10.1	0.19	0.71	–0.0023	No	–0.17
S2	Sea ice in shear zone off Devon Island	195	–10.7	0.26	1.40	0.0005	No	–0.50
S3	Sea ice in shear zone between S2 and S4	50	–9.6	0.28	0.77	–0.0019	No	–0.86
S4	Sea ice in shear zone off Ward Point	143	–11.9	0.26	0.93	–0.0095	Yes	–0.24

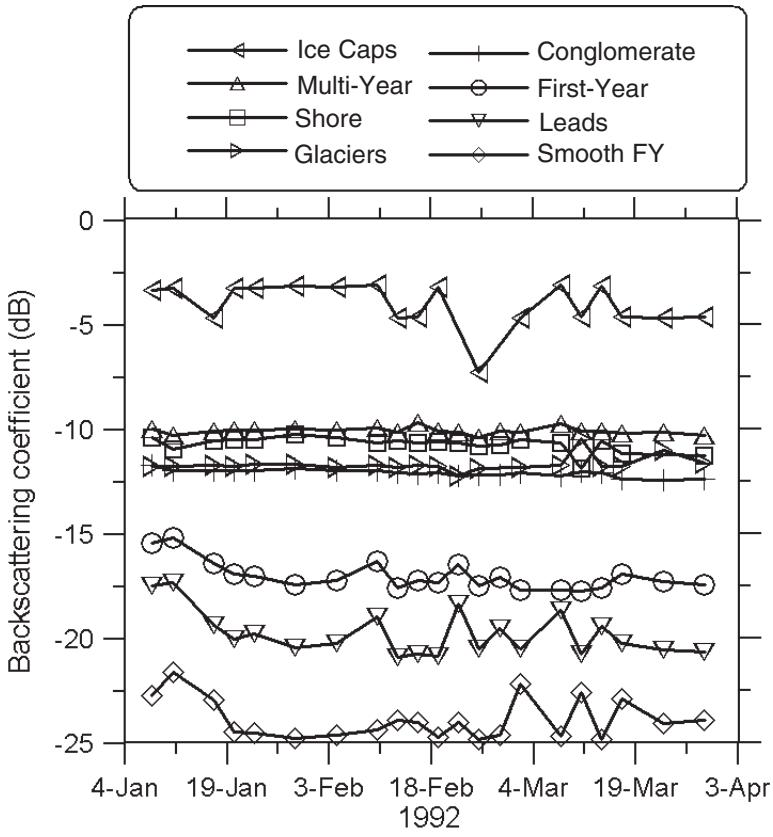

Fig. 4 Backscatter time series for six sea-ice and two land-ice types.

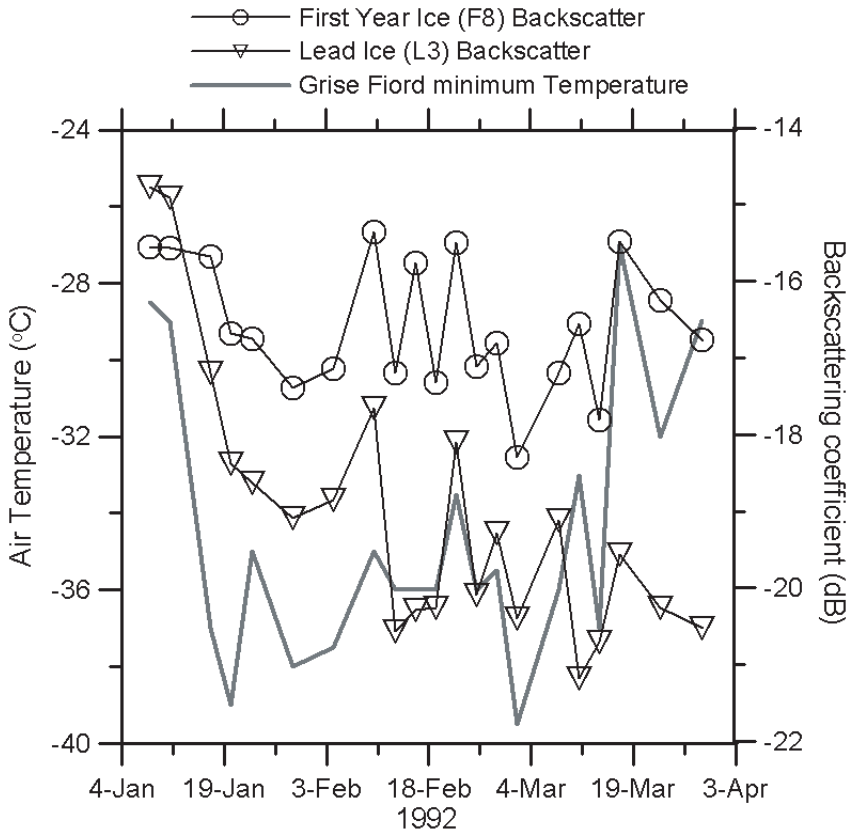

Fig. 5 Air temperature of Grise Fiord plotted along with the backscatter of first-year ice and lead ice backscatter over a 3-month period.

backscatter variability in Lady Ann Strait: both are reversible, and both will act to increase backscatter when temperatures are higher.

Increases in temperatures at the snow/ice interface can be caused by two synoptic mechanisms: advection of warm air masses, and changes in the downwelling longwave radiation flux caused by clouds associated with synoptic activity (Steffen and DeMaria, 1996). Fraser (1983) describes both conditions as being associated with low-pressure systems that either move into or are formed in Baffin Bay. These storm systems are separated by intervals of about seven days for the Baffin Bay region according to Steffen (1985), which is close to the observed backscatter modulation for the Lady Ann Strait first-year ice samples (Fig. 5).

3 LEAD ICE (L1-4)

Seven regions were selected from refrozen leads in first-year ice. The refrozen leads were identified as linear features of lower backscatter, which does exclude newly, refrozen leads with frost flowers, having a high backscatter signal. The mean backscatter of the samples ranges from –18.5 dB to –20.6 dB (Table 1), lower than the first-year samples.

The temporal backscatter variability of the lead ice samples (standard deviations from 0.64 dB to 1.76 dB between sites) is generally higher than the first-year samples, but considerable overlap exists. Barber et al. (1995) found that the variability of first-year ice in late winter and spring was greater for thinner ice resulting from warmer spring temperatures. The correlation between lead ice backscatter values and Grise Fiord air temperatures is similar to that between first-year ice and temperature (Table 1), although the magnitude of the correlations is lower, and negative trends of backscatter with time exist for the lead ice regions, similar to first-year ice.

The positive correlation of air temperature with the lead ice through time suggests that similar processes govern the backscatter of first-year ice and lead ice at the base, i.e., the build up of brine at the base of the snow pack. Two significant differences exist: (a) the backscatter of lead ice is lower and (b) lead ice is more sensitive to temperature fluctuations (Fig. 5). The most important factor contributing to the low backscatter of lead ice is its smooth surface.

4 LOW BACKSCATTER FIRST-YEAR ICE (D1-2)

In the SAR images, a number of small features with very low backscatter were noticed. This “low backscattering ice” was found in Brae Bay (Fig. 6). Samples D1 and D2 have the lowest mean backscatter of any sample regions, ranging from –22.5 dB to –23.7 dB. Such low backscatter values have been observed only for calm open water and grease ice (Steffen and Heinrichs, 1994). Both of these classes are unlikely to be present in landfast ice. Sea ice that is protected from shear and stress during freeze-up has a very smooth surface, and consequently has a low backscatter value. The temporal variability of these samples is quite high, with a standard deviation

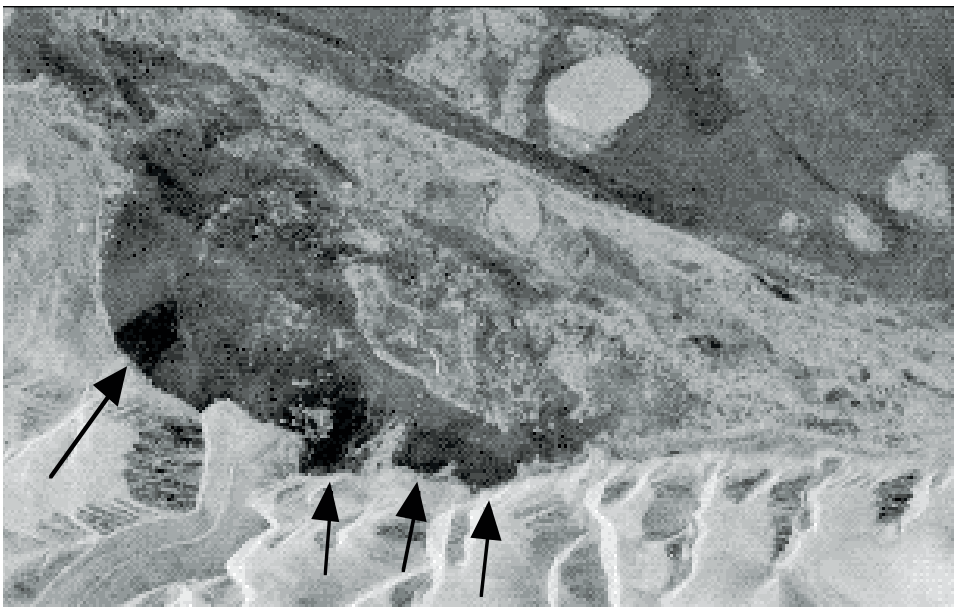

Fig. 6 A portion of an ERS-1 SAR image of Lady Ann Strait acquired on 15 February 1992 (© European Space Agency, 1992). This image shows Brae Bay and the sites for the smooth first-year ice in embayments along the coast. The area covered by the image is approximately 30.5 km by 19 km.

between 0.85 dB and 1.14 dB (Table 1). The pattern of temporal backscatter variability shows some similarities to other records shown in Fig. 4. We suggest that this surface is smooth, first-year ice, based on the locations and backscatter characteristics of this ice.

5 CONGLOMERATE ICE (C1-4)

The conglomerate ice samples (C1–C4) have the appearance of composites of multiple ice types (Fig. 7). The samples have mean backscatter values ranging from –10.5 dB to –13.8 dB (Table 1), slightly lower than the multi-year samples, but higher than the first-year samples. The conglomerate samples show low temporal backscatter variability (temporal standard deviations from 0.14 dB to 0.24 dB, spatial standard deviation 0.88 dB to 1.22 dB), which partially overlaps the range of the multi-year samples, and is lower than any of the first-year samples. There is no correlation of conglomerate ice backscatter with air temperature. Single-pixel sampling shows that many of the rounded ice pieces within the conglomerate have backscatter values typical of multi-year ice, while the matrix in which the pieces are imbedded is similar to the first-year samples. An apparent explanation is that the conglomerate ice is a combination of both first- and second-year ice.

6 LANDFAST SHORE ICE (S1-4)

One of the features that stands out in the SAR images is the landfast shore ice, a band of highly backscattering sea ice along the northern and eastern shore of Devon Island (Fig. 2). Four samples were chosen along the Devon Island coast. The mean backscatter of these samples ranges from –9.6 to –11.9 dB (Table 1), which overlaps with the multi-year ice samples, but not with the first-year samples. The backscatter of the near-shore samples exhibits standard deviations ranging from 0.19 to 0.27 dB. This is slightly higher than the multi-year samples, but much less than the first-year samples. Despite the similarity of the samples in backscatter and its variability with multi-year ice, it is quite obvious from their appearance that these samples do not represent multi-year ice. Rather, we propose that this surface is composed of highly deformed first-year ice (sometimes called a rubble field). An empirically tested model of the backscatter from deformed sea ice (Carlström and Ulander, 1995) predicts that ERS-1 SAR backscatter of saline ice with an average block size of 0.2 m will range from –8 to –11 dB. This is consistent with our observations. The backscatter of all of the shore ice samples is anticorrelated with Grise Fiord temperature, with sample S3 having a correlation coefficient of –0.86. The only other ice samples with a consistenttly negative correlation are the multi-year samples. Three of the samples have a decreasing backscatter trend, and the trend for S4 is statistically significant and of about the same magnitude as the trends for the conglomerate ice. We suggest that the sampled shore ice is less saline than the other first-year ice types, having been formed earlier (Steffen and DeMaria, 1996), and therefore exhibits a backscatter response closer to that of multi-year ice.

4 Discussion and conclusion

In this study, ERS-1 SAR data were combined with in situ meteorological data (air temperatures) to examine sea- and land-ice backscatter in Lady Ann Strait and Jones Sound during winter. Temporal backscattering coefficient means, stan-

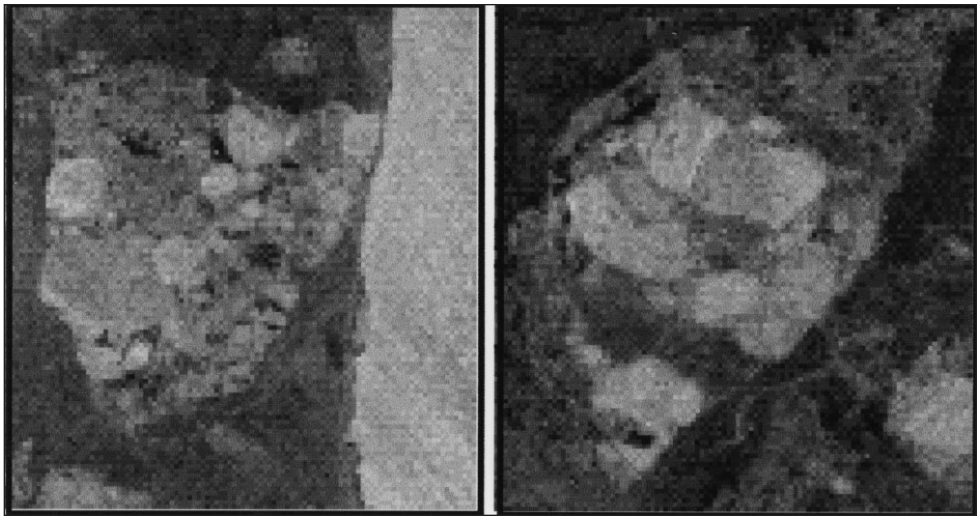

Fig. 7 Two portions of an ERS-1 SAR image of Lady Ann Strait taken on 15 February 1992 (© European Space Agency, 1992). These images show two typical areas of conglomerate ice in Jones Sound. The areas covered by the images are approximately 11 km by 11 km.

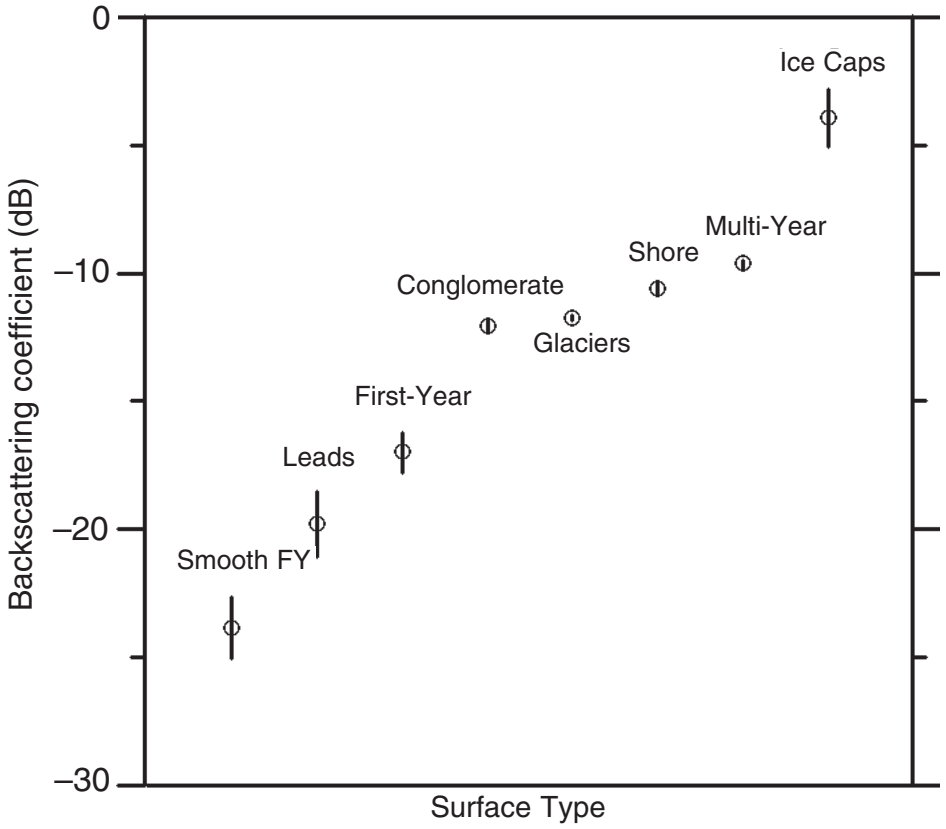

Fig. 8 Mean (circle) and standard deviation (vertical line) of backscatter for six sea-ice and two land-ice types over a 3-month period (January–March 1992).

dard deviations, and trends were calculated for twenty-eight sample regions belonging to eight land- and sea-ice types. The mean backscatter (±standard deviation) for the eight different ice surfaces identified in the ERS-1 C-band SAR images are shown in Fig. 8.

Ice caps in general exhibit the highest backscatter value (σ^{o}_{mean} = –3.9 dB) found for natural surfaces. The Devon Island ice cap samples show a high temporal variability possibly related to the formation of surface hoar. Sudden drops in backscatter values of up to 5 dB were not uncommon between

individual images. Valley glacier ice has the most stable backscatter value over time with the smallest observed standard deviations of 0.08–0.10 dB. The backscatter value of glaciers and ice caps is not affected by variations in air temperature. The calibration accuracy of ERS-1 backscatter is established at 1.0 dB for the ASF processor. This analysis shows that the ERS-1 SAR performs within that accuracy or better over the three months of our study. We suggest using the backscatter signature of valley glacier ice during winter to assess the temporal scatter drift over the lifespan of the satellite. However, valley glacier backscatter signatures must be obtained from the same altitude for such a comparison, because backscatter increases with altitude.

Sea ice can be classified in two broad categories according to their temporal backscatter behaviour:

(a) first-year ice, lead ice, and smooth first-year ice which show a positive correlation with air temperature, and a negative trend over the 90-day period. The positive correlation of first-year ice backscatter with Grise Fiord temperature is likely a result of an increase in brine volume in the lower portions of the snow pack with increasing temperature. There is a time lag of up to three days between backscatter variations and changes in air temperature, caused by the insulating effect of the snow cover. For lead ice, the magnitude of the temperature-backscatter correlations is lower. We attribute this to the smoother ice surface.
(b) multi-year ice, conglomerate ice, and shore ice, which have no temporal backscatter trend over the 90-day period (Table 1), and no correlation with air temperature. For multi-year ice, this behaviour can be explained by dominant volume scattering from small gas bubbles in multi-year ice. Multi-year ice has the highest mean backscatter (σ^o_{mean} = –9.6 dB) and lowest variability of all sea-ice types studied. Conglomerate ice and shore ice both have lower mean backscatter values (σ^o_{mean} = –12.03 dB, σ^o_{mean} = –10.58 dB respectively) with standard deviations ranging from 0.14 to 0.28 dB (Fig. 8).

Knowledge of the temporal backscatter variability for glacier and sea-ice types can greatly improve future SAR ice classifiers. In order to monitor variations in the extent and types of land and sea ice in polar regions over time, we need to continue constraining the backscatter characteristics of these surfaces under varying climatic conditions. Such studies also give insight into the processes at the ocean-atmosphere and ice-atmosphere interfaces. Future work ought to focus on acquiring more highly resolved temporal records of SAR imagery, meteorological observations, field measurements, and snow depth in particular.

Acknowledgments

This research was funded under contract NAGW-4978 by the National Aeronautics and Space Administration (NASA) Ocean Science Branch. The ASF at the University of Alaska in Fairbanks is acknowledged with gratitude for the processing and delivery of the ERS-1 SAR scenes. The MSC was very helpful in providing the Grise Fiord temperature values. We also acknowledge Dr. Valerie Sloan for her review and editorial help.

References

BARBER, D.G.; T. PAPAKYRIAKOU, E.F. LEDREW AND M.E. SHOKR. 1995. An examination of the relation between the spring period evolution of the scattering coefficient (σ^0) and radiative fluxes over landfast ice. *Int. J. Rem. Sens.* **16**(**17**): 3343–3363.

CARLSTRÖM, A. and L.M.H. ULANDER. 1995. Validation of backscatter models for level and undeformed sea-ice in ERS-1 SAR images. *Int. J. Rem. Sens.* **16**(**17**): 3245–3266.

COLBECK, S.C. 1988. On the micrometeorology of surface hoar growth on snow in mountainous area. *Boundary-Layer Meteorol.* **44**: 1–12.

DRINKWATER, M.R. and G.B. CROCKER. 1998. Modelling Changes in the Dielectric and Scattering Properties of Young Snow-Covered Sea Ice at GHz Frequencies. *J. Glaciol.* **34**(**118**): 274–282.

FAHNESTOCK, M.; R. BINDSCHADLER, R. KWOK and R. JEZEK. 1993. Greenland ice sheet surface properties and ice dynamics from ERS-1 SAR imagery. *Science*, **262**: 1530–1534.

FRASER, D. 1983. Climate of northwestern Baffin Bay and Lancaster Sound. Environmental Studies No. 29, Indian and Northern Affairs Canada, Ottawa. 93 pp.

HACHIKUBO, A. and E. AKITAYA. 1997. Effect of wind on surface hoar growth on snow. *J. Geophys. Res.* **102**: 4367–4373.

HALLIKAINEN, M. and D. WINEBRENNER. 1992. The physical basis for sea ice remote sensing. In: *Microwave Remote Sensing of Sea Ice*, F. Carsey (Ed.), Geophys. Monogr. Ser. Vol. 68, AGU, Washington, D.C., pp. 29–46.

JEZEK, K.C.; M.R. DRINKWATER, J.P. CRAWFORD, R. BINDSCHADLER and R. KWOK. 1993. Analysis of synthetic aperture radar data collected over the southwestern Greenland ice sheet. *J. Glaciol.* **39**(**131**): 119–132.

———; P. GOGINENI and M. SHANABLEH. 1994. Radar measurements of melt zones on the Greenland Ice Sheet. *Geophys. Res. Lett.* **21**(**1**): 33–36.

KWOK, R. and G.F. CUNNINGHAM. 1994. Backscatter characteristics of the winter ice cover in the Beaufort Sea. *J. Geophys. Res.* **99**: 7187–7802.

MÜLLER, F.; P. BERGER, H. ITO, A. OHMURA, K. SCHROFF and K. STEFFEN. 1979. North Water Project, Report VI, Swiss Federal Institute of Technology, Dept. of Geography, Zürich, Switzerland, pp. 123.

ONSTOTT, R. 1992. SAR and scatterometer signatures of sea ice. In: *Microwave Remote Sensing of Sea Ice*, F. Carsey (Ed.), Geophys. Monogr. Ser. Vol. 68, AGU, Washington, D.C., pp. 73–104.

PARTINGTON, K.C. 1998. Discrimination of Glacier Facies using Multi-Temporal SAR Data. *J. Glaciol.* **44**: 42–53.

REES, W.G.; J.A. DOWDESWELL and A.D. DIAMENT. 1995. Analysis of ERS-1 Synthetic Aperture Radar data from Nordaustlandet, Svalbard. *Int. J. Rem. Sens.* **16**(**5**): 905–924.

RIGNOT, E. 1995. Backscatter model for the unusual radar properties of the Greenland Ice Sheet. *J. Geophys. Res.* 100: 9389–9400.

SCHUCHMANN, R.A.; C.C. WACKERMAN and L.L. SUTHERLAND. 1991. The use of synthetic aperture radar to map the polar oceans, Environmental Science Institute of Michigan. Ann Arbor, 316 pp.

SHOKR, M. 1998. Field observations and model calculations of dielectric properties of Arctic sea ice in the microwave C-band. *IEEE Trans. Geosci. Remote Sens*. **36**(**2**): 463–478.

STEFFEN, K. 1985. Warm water in the North Water, northern Baffin Bay during winter. *J. Geophys. Res*. **90**: 9129–9136.

——— and J. HEINRICHS. 1994. Feasibility of sea ice typing with synthetic aperture radar (SAR): Merging of Landsat Thematic Mapper and ERS 1

SAR satellite imagery. *J. Geophys. Res.* **99**: 22413–22424.

——— and T. DEMARIA. 1996. Surface energy fluxes of Arctic winter sea ice in Barrow Strait. *J. Appl. Meteorol.* **35**: 2067–2079.

SWIFT, C.T.; K. ST. GERMAIN, K.C. JEZEK, S.P. GOGENINI, A.J. GOW, D.K. PEROVICH, T.C. GRENFELL and R.G. ONSTOTT. 1992. Laboratory investigations of the electromagnetic properties of artificial sea ice. In: *Microwave Remote Sensing of Sea Ice*, F. Carsey (Ed.), Geophys. Monogr. Ser. Vol. 68, AGU, Washington, D.C. pp. 177–200.

ULANDER, L.M.H.; A. CARLSTRÖM and J. ASKNE. 1995. Effect of frost flowers, rough saline snow and slush on the ERS-1 SAR backscatter of thin Arctic sea-ice. *Int. J. Rem. Sens.* **16**: 3287–3305.

WILLIAMS, J. 1996. ASF Calibration Presentation, Alaska SAR Facility, University of Alaska Fairbanks, 24 October 1996. 120 pp.